Manual to the opacity tables

Chris Ormel

August 30, 2013

Summary of changes

September 2013:

- Corrected for a bug in the calculation of the particle-averaged asymmetry factor
  (credits to Amy Stutz and Will Fisher for pointing this out)

February 2013:

- Increased number of wavelength grid points to 500;
- All data are averaged over size distribution;
- Computed the full scattering phase matrix;
- Corrected for a previously incorrect treatment of the graphite component in the opacity calculations;

Earlier:

- In cases with ice mantles, no longer included the ice in the calculation of the dust opacities. Opacities are henceforth given in cm^2 per unit mass silicates and graphite.

1 Dust models

The opacity data are given for four models, corresponding to Fig. 6 of Ormel et al. (2011). These dust size and porosity distribution was calculated in Ormel et al. (2009) for two cases: ice-coated grains and bare grains. Since ice has much better sticking properties to counteract the high-velocity collisions, larger aggregates form, where the bare grain distribution will settle into a steady-state.

Given these distribution, four models are constructed by 'mixing' silicate, graphite, and ice material, as summarised in this table:

Name	# spatial components (Type-I mixing)		#Aggregate components (Type-II mixing)		Silicate/graphite fraction
		size distribution		component 1	component 2	
(sil,gra)	1	bare	2	silicate	graphite	1
(ic-sil,ic-gra)	1	ices	2	ic-silicate	ic-graphite	0.73
(ic-sil,gra)	1	ices	2	ic-silicate	graphite	0.82
ic-sil+gra	2	–ices	1	ic-silicate		0.82
		–bare	1	graphite		

In the first three models silicates and graphite grains are mixed within the aggregates. This is referred to as 'Type-II' mixing (Ormel et al. 2011). In the final `ic-sil+gra` model the dust consist of a spatial mixture of aggregates made out of either silicate or graphite materials (type-I mixing). Occasionally, silicates and graphite grains are assumed to be ice-coated ('ic' = ice-coated), in which case the coating layer is assumed to be 10% in radius.

Note on dust masses: The total silicates:graphite abundance is always 2:1 in the above models. The total dust abundance is 1/100 of the gas abundance, which is $\rho_{gas} = 10^5$ cm^{-3} $\times 2.34 m_{amu}$, where m_{amu} is the atomic mass unit. In Ormel et al. (2011) we included the ice layers in calculating the opacity per unit mass. This is no longer done, however; opacities are since calculated per unit gram dust (graphite and silicates only), not counting the mass in the ice coating. This implies a somewhat larger opacity (in case of an ice coating) with respect to (Ormel et al. 2011). For example, in the fully ice-coated

(ic-sil,ic-gra) model 73% of the solid mass is in dust and 27% in ice, which meant that in this model we now use a dust density of $\rho_{\text{dust}} = 0.73\rho_{\text{gas}}/100$. [1]

2 Data Tables

The opacity tables come in two flavours:

1. A summary of the key distribution-averaged quantities. These files are denoted `NameTopc.txt`, where T is the time indicator.
2. The full phase matrix P_{ij} tables. These are the files `NameTPij.txt`.

The time indicator number T refers to the dust size distribution, which evolves due to coagulation and fragmentation processes (Ormel et al. 2009), after a physical time t:

T	Dust Size distribution after coagulating for
1	0.03 Myr
2	0.1 Myr
3	0.3 Myr
4	1.0 Myr
5	3.0 Myr
6	10. Myr

The calculation also provides the porosity of the dust particles; that is, the internal density of dust particles is evolving as well.

2.1 Extinction cross section tables

For each of these times the file `NameTopc.txt` provides the distribution-averaged opacities as function of wavelength:

```
#cols::[lambda,kappa-ext,kappa-sca,kappa-back,gsca]
#colunits::[cm,cm2/g,cm2/g,cm2/g,]
    (1)         (2)         (3)         (4)         (5)
    1.000E-05   8.40E+04    4.41E+04    4.46E+03    8.29E-01
```

Where the columns denote: (1) λ, wavelength in cm; (2) κ_{ext}, total extinction cross section in cm^2 per unit gram dust; (3) κ_{sca}, scattering cross section per unit gram dust; (4) κ_{back} back scattering cross section per unit gram dust; (5) $g = \langle\cos\theta\rangle$, asymmetry factor.

These are distribution-averaged quantities. For the opacities they are calculated

$$\kappa_i(\lambda) = \frac{1}{\rho_{\text{dust}}} \int \frac{dn}{da} \sigma_i(a, \lambda)\, \mathrm{d}a, \tag{1}$$

where dn/da is the size distribution and $\sigma_i(a, \lambda)$ the opacity of a single particle of size a_i at wavelength λ. The distribution-averaged absorption coefficient κ_{abs} follows from $\kappa_{\text{abs}} = \kappa_{\text{ext}} - \kappa_{\text{sca}}$.

The distribution-average asymmetry factor is calculated as:

$$\overline{g}(\lambda) = \frac{1}{\beta_{\text{sca}}} \int \frac{dn}{da} g(a, \lambda)\, \mathrm{d}a \tag{2}$$

where $\beta_{\text{sca}} = \kappa_{\text{sca}}\rho_{\text{dust}}$ is the scattering cross section per unit volume.

2.2 Phase matrix tables

The files `NameTP11.txt`, `NameTP12.txt`, `NameTP33.txt` and `NameTP34.txt` contain the full phase matrix table as function of scattering angle θ (columns) and wavelength λ (rows). For example:

```
#cols::[lambda,P11(theta)]
    (0)         (1)       (2)                    (181)
    1.000E-05   6.46E+01  6.42E+01    ...  9.97E-02  9.96E-02
```

---

[1]Obviously, the more self-consistent treatment would have been to adopt a larger monomer radius in the aggregation models of Ormel et al. 2009, which was not done. However, since the mantles are small, the procedure applied here is reasonable).
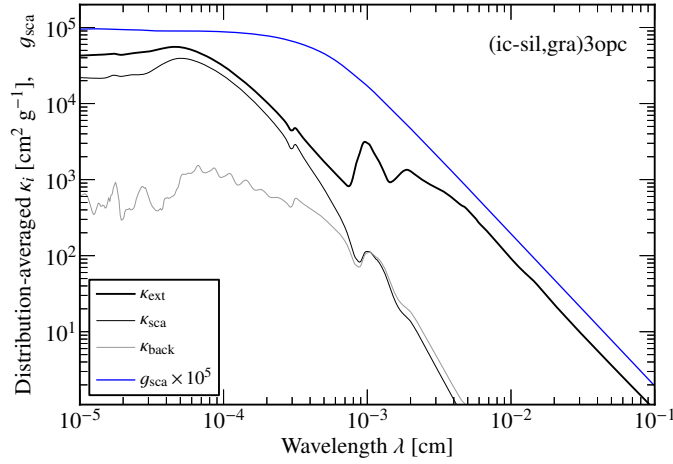
Figure 1: Size distribution-averaged opacities and the distribution-averaged asymmetry factor (multiplied by 10^5) for the `(ic-sil,gra)3opc` model.

Column (0) again denotes the wavelength in cm. The remainder columns i (where i runs from 1 to 181) denote the phase matrix $P_{11}(\theta_i)$ where $\theta_i = (i - 1)$ is in degrees.

Properties of the phase matrix. Note the following properties/definitions of the phase matrix:

$$\int_\Omega d\theta \, P_{11}(\theta) d\Omega = 4\pi; \qquad \frac{\mathbf{P}_{ij}}{4\pi r^2} = \frac{1}{\beta_{\text{sca}}} \int da \frac{dn}{da} \mathbf{M}_{ij} \qquad (3)$$

where $\mathbf{M}_{ij}$, the transformation matrix of a single sphere, relates the incoming to the outgoing elements of a Stokes vector, *i.e.,* $(I, Q, U, V) = \mathbf{M}(I_0, Q_0, U_0, V_0)$ (van de Hulst 1981). The integration is over the size distribution $n(a) = dn/da$, r is the radial distance from the particle, and β_{sca} is the scattering opacity per unit volume, averaged over the distribution, $\beta_{\text{sca}} = \kappa_{\text{sca}}/\rho_{\text{dust}}$. For spherical particles we have

$$\mathbf{P}_{ij}(\theta) = \begin{pmatrix} P_{11} & P_{12} & 0 & 0 \\ P_{12} & P_{11} & 0 & 0 \\ 0 & 0 & P_{33} & -P_{34} \\ 0 & 0 & P_{34} & P_{33} \end{pmatrix} \qquad (4)$$

So only these four independent elements are provided. For a single sphere, the transformation matrix elements follow from the scattering matrices $S_1(\theta), S_2(\theta)$:

$$M_{11} = \frac{1}{(kr)^2} \frac{S_2(\theta)S_2^*(\theta) + S_1(\theta)S_1^*(\theta)}{2} \qquad (5)$$

$$M_{12} = \frac{1}{(kr)^2} \frac{S_2(\theta)S_2^*(\theta) - S_1(\theta)S_1^*(\theta)}{2} \qquad (6)$$

$$M_{33} = \frac{1}{(kr)^2} \frac{S_2^*(\theta)S_1(\theta) + S_1(\theta)S_2^*(\theta)}{2} \qquad (7)$$

$$M_{34} = \frac{1}{(kr)^2} \frac{S_2^*(\theta)S_1(\theta) - S_2(\theta)S_1^*(\theta)}{2i} \qquad (8)$$

where $k = 2\pi/\lambda$. The single-particle scattering matrices $S_1(\theta), S_2(\theta)$ follow directly from Mie theory.

3 Figures

Figure 1 gives the extinction, scattering, and back scattering opacities of the `(ic-sil,gra)3opc` model. These are distribution-averaged quantities. It also gives the distribution-averaged asymmetry factor, which is multiplied by a factor 10^5 for clarity. Figure 2 plots the extinction κ_{ext} as function of wavelength for all four models. Compared to the corresponding Fig. 6 in Ormel et al. (2011) small differences may be noticed. This was due to an incorrect treatment of the way graphite (which is an anisotropic material) and the normalization to the dust mass (now without counting the ice).
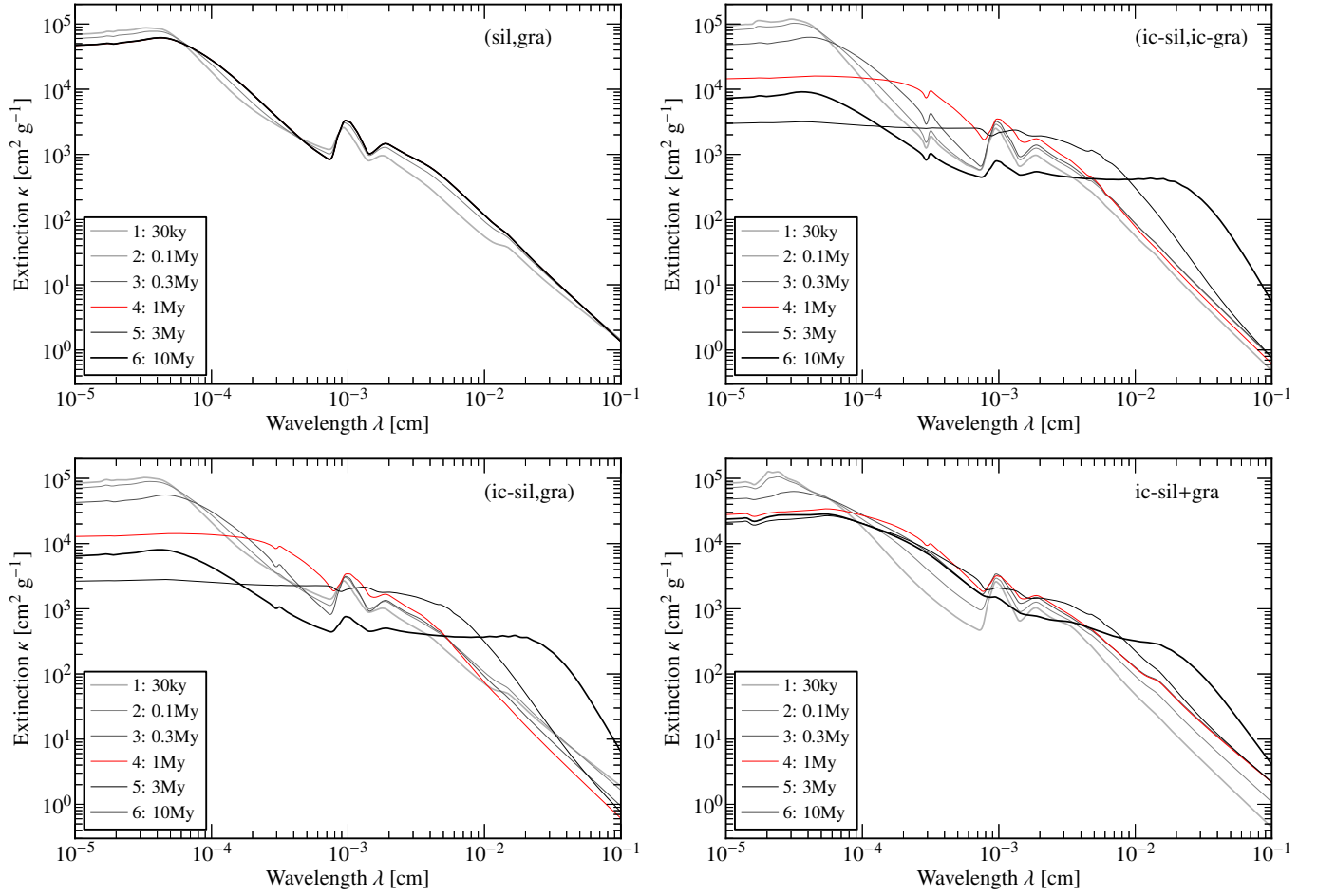
3

Figure 2: Plots of the distribution-averaged extinction as function of wavelength, $\kappa_{ext}(\lambda)$, for the four distribution/coagulation models.

References

Ormel, C. W., Min, M., Tielens, A. G. G. M., Dominik, C., & Paszun, D. 2011, A&A, 532, A43

Ormel, C. W., Paszun, D., Dominik, C., & Tielens, A. G. G. M. 2009, A&A, 502, 845

van de Hulst, H. C. 1981, Light scattering by small particles, ed. H. C. van de Hulst